First Observation of the $M1$ Transition $\psi(3686) \to \gamma\eta_c(2S)$

M. Ablikim,[1] M. N. Achasov,[5] D. J. Ambrose,[40] F. F. An,[1] Q. An,[41] Z. H. An,[1] J. Z. Bai,[1] Y. Ban,[27] J. Becker,[2] N. Berger,[1] M. Bertani,[18] J. M. Bian,[39] E. Boger,[20,*] O. Bondarenko,[21] I. Boyko,[20] R. A. Briere,[3] V. Bytev,[20] X. Cai,[1] A. Calcaterra,[18] G. F. Cao,[1] J. F. Chang,[1] G. Chelkov,[20,*] G. Chen,[1] H. S. Chen,[1] J. C. Chen,[1] M. L. Chen,[1] S. J. Chen,[25] Y. Chen,[1] Y. B. Chen,[1] H. P. Cheng,[14] Y. P. Chu,[1] D. Cronin-Hennessy,[39] H. L. Dai,[1] J. P. Dai,[1] D. Dedovich,[20] Z. Y. Deng,[1] A. Denig,[19] I. Denysenko,[20,†] M. Destefanis,[44] W. M. Ding,[29] Y. Ding,[23] L. Y. Dong,[1] M. Y. Dong,[1] S. X. Du,[47] J. Fang,[1] S. S. Fang,[1] L. Fava,[44,‡] F. Feldbauer,[2] C. Q. Feng,[41] R. B. Ferroli,[18] C. D. Fu,[1] J. L. Fu,[25] Y. Gao,[36] C. Geng,[41] K. Goetzen,[7] W. X. Gong,[1] W. Gradl,[19] M. Greco,[44] M. H. Gu,[1] Y. T. Gu,[9] Y. H. Guan,[6] A. Q. Guo,[26] L. B. Guo,[24] Y. P. Guo,[26] Y. L. Han,[1] X. Q. Hao,[1] F. A. Harris,[38] K. L. He,[1] M. He,[1] Z. Y. He,[26] T. Held,[2] Y. K. Heng,[1] Z. L. Hou,[1] H. M. Hu,[1] J. F. Hu,[6] T. Hu,[1] B. Huang,[1] G. M. Huang,[15] J. S. Huang,[12] X. T. Huang,[29] Y. P. Huang,[1] T. Hussain,[43] C. S. Ji,[41] Q. Ji,[1] X. B. Ji,[1] X. L. Ji,[1] L. K. Jia,[1] L. L. Jiang,[1] X. S. Jiang,[1] J. B. Jiao,[29] Z. Jiao,[14] D. P. Jin,[1] S. Jin,[1] F. F. Jing,[36] N. Kalantar-Nayestanaki,[21] M. Kavatsyuk,[21] W. Kuehn,[37] W. Lai,[1] J. S. Lange,[37] J. K. C. Leung,[35] C. H. Li,[1] Cheng Li,[41] Cui Li,[41] D. M. Li,[47] F. Li,[1] G. Li,[1] H. B. Li,[1] J. C. Li,[1] K. Li,[10] Lei Li,[1] N. B. Li,[24] Q. J. Li,[1] S. L. Li,[1] W. D. Li,[1] W. G. Li,[1] X. L. Li,[29] X. N. Li,[1] X. Q. Li,[26] X. R. Li,[28] Z. B. Li,[33] H. Liang,[41] Y. F. Liang,[31] Y. T. Liang,[37] G. R. Liao,[36] X. T. Liao,[1] B. J. Liu,[34] B. J. Liu,[1] C. L. Liu,[3] C. X. Liu,[1] C. Y. Liu,[1] F. H. Liu,[30] Fang Liu,[1] Feng Liu,[15] H. Liu,[1] H. B. Liu,[6] H. H. Liu,[13] H. M. Liu,[1] H. W. Liu,[1] J. P. Liu,[45] K. Y. Liu,[23] Kai Liu,[6] Kun Liu,[27] P. L. Liu,[29] S. B. Liu,[41] X. Liu,[22] X. H. Liu,[1] Y. Liu,[1] Y. B. Liu,[26] Z. A. Liu,[1] Zhiqiang Liu,[1] Zhiqing Liu,[1] H. Loehner,[21] G. R. Lu,[12] H. J. Lu,[14] J. G. Lu,[1] Q. W. Lu,[30] X. R. Lu,[6] Y. P. Lu,[1] C. L. Luo,[24] M. X. Luo,[46] T. Luo,[38] X. L. Luo,[1] M. Lv,[1] C. L. Ma,[6] F. C. Ma,[23] H. L. Ma,[1] Q. M. Ma,[1] S. Ma,[1] T. Ma,[1] X. Y. Ma,[1] Y. Ma,[11] F. E. Maas,[11] M. Maggiora,[44] Q. A. Malik,[43] H. Mao,[1] Y. J. Mao,[27] Z. P. Mao,[1] J. G. Messchendorp,[21] J. Min,[1] T. J. Min,[1] R. E. Mitchell,[17] X. H. Mo,[1] C. Morales Morales,[11] C. Motzko,[2] N. Yu. Muchnoi,[5] Y. Nefedov,[20] C. Nicholson,[6] I. B. Nikolaev,[5] Z. Ning,[1] S. L. Olsen,[28] Q. Ouyang,[1] S. Pacetti,[18,§] J. W. Park,[28] M. Pelizaeus,[38] H. P. Peng,[41] K. Peters,[7] J. L. Ping,[24] R. G. Ping,[1] R. Poling,[39] E. Prencipe,[19] C. S. J. Pun,[35] M. Qi,[25] S. Qian,[1] C. F. Qiao,[6] X. S. Qin,[1] Y. Qin,[27] Z. H. Qin,[1] J. F. Qiu,[1] K. H. Rashid,[43] G. Rong,[1] X. D. Ruan,[9] A. Sarantsev,[20,‖] B. D. Schaefer,[17] J. Schulze,[2] M. Shao,[41] C. P. Shen,[38,¶] X. Y. Shen,[1] H. Y. Sheng,[1] M. R. Shepherd,[17] X. Y. Song,[1] S. Spataro,[44] B. Spruck,[37] D. H. Sun,[1] G. X. Sun,[1] J. F. Sun,[12] S. S. Sun,[1] X. D. Sun,[1] Y. J. Sun,[41] Y. Z. Sun,[1] Z. J. Sun,[1] Z. T. Sun,[41] C. J. Tang,[31] X. Tang,[1] E. H. Thorndike,[40] H. L. Tian,[1] D. Toth,[39] M. Ullrich,[37] G. S. Varner,[38] B. Wang,[9] B. Q. Wang,[27] K. Wang,[1] L. L. Wang,[4] L. S. Wang,[1] M. Wang,[29] P. Wang,[1] P. L. Wang,[1] Q. Wang,[1] Q. J. Wang,[1] S. G. Wang,[27] X. F. Wang,[12] X. L. Wang,[41] Y. D. Wang,[41] Y. F. Wang,[1] Y. Q. Wang,[29] Z. Wang,[1] Z. G. Wang,[1] Z. Y. Wang,[1] D. H. Wei,[8] P. Weidenkaff,[19] Q. G. Wen,[41] S. P. Wen,[1] M. Werner,[37] U. Wiedner,[2] L. H. Wu,[1] N. Wu,[1] S. X. Wu,[41] W. Wu,[26] Z. Wu,[1] L. G. Xia,[36] Z. J. Xiao,[24] Y. G. Xie,[1] Q. L. Xiu,[1] G. F. Xu,[1] G. M. Xu,[27] H. Xu,[1] Q. J. Xu,[10] X. P. Xu,[32] Y. Xu,[26] Z. R. Xu,[41] F. Xue,[15] Z. Xue,[1] L. Yan,[41] W. B. Yan,[41] Y. H. Yan,[16] H. X. Yang,[1] T. Yang,[9] Y. Yang,[15] Y. X. Yang,[8] H. Ye,[1] M. Ye,[1] M. H. Ye,[4] B. X. Yu,[1] C. X. Yu,[26] J. S. Yu,[22] L. Yu,[15,**] S. P. Yu,[29] C. Z. Yuan,[1] W. L. Yuan,[24] Y. Yuan,[1] A. A. Zafar,[43] A. Zallo,[18] Y. Zeng,[16] B. X. Zhang,[1] B. Y. Zhang,[1] C. C. Zhang,[1] D. H. Zhang,[1] H. H. Zhang,[33] H. Y. Zhang,[1] J. Zhang,[24] J. G. Zhang,[12] J. Q. Zhang,[1] J. W. Zhang,[1] J. Y. Zhang,[1] J. Z. Zhang,[1] L. Zhang,[25] S. H. Zhang,[1] T. R. Zhang,[24] X. J. Zhang,[1] X. Y. Zhang,[29] Y. Zhang,[1] Y. H. Zhang,[1] Y. S. Zhang,[9] Z. P. Zhang,[41] Z. Y. Zhang,[45] G. Zhao,[1] H. S. Zhao,[1] J. W. Zhao,[1] K. X. Zhao,[24] Lei Zhao,[41] Ling Zhao,[1] M. G. Zhao,[26] Q. Zhao,[1] S. J. Zhao,[47] T. C. Zhao,[1] X. H. Zhao,[25] Y. B. Zhao,[1] Z. G. Zhao,[41] A. Zhemchugov,[20,*] B. Zheng,[42] J. P. Zheng,[1] Y. H. Zheng,[6] Z. P. Zheng,[1] B. Zhong,[1] J. Zhong,[2] L. Zhou,[1] X. K. Zhou,[6] X. R. Zhou,[41] C. Zhu,[1] K. Zhu,[1] K. J. Zhu,[1] S. H. Zhu,[1] X. L. Zhu,[36] X. W. Zhu,[1] Y. M. Zhu,[26] Y. S. Zhu,[1] Z. A. Zhu,[1] J. Zhuang,[1] B. S. Zou,[1] J. H. Zou,[1] and J. X. Zuo[1]

(BESIII Collaboration)

[1]*Institute of High Energy Physics, Beijing 100049, People's Republic of China*
[2]*Bochum Ruhr-University, 44780 Bochum, Germany*
[3]*Carnegie Mellon University, Pittsburgh, Pennsylvania 15213, USA*
[4]*China Center of Advanced Science and Technology, Beijing 100190, People's Republic of China*
[5]*G. I. Budker Institute of Nuclear Physics SB RAS (BINP), Novosibirsk 630090, Russia*
[6]*Graduate University of Chinese Academy of Sciences, Beijing 100049, People's Republic of China*
[7]*GSI Helmholtzcentre for Heavy Ion Research GmbH, D-64291 Darmstadt, Germany*
[8]*Guangxi Normal University, Guilin 541004, People's Republic of China*
[9]*GuangXi University, Nanning 530004, People's Republic of China*

[10]Hangzhou Normal University, Hangzhou 310036, People's Republic of China
[11]Helmholtz Institute Mainz, D 55099 Mainz, Germany
[12]Henan Normal University, Xinxiang 453007, People's Republic of China
[13]Henan University of Science and Technology, Luoyang 471003, People's Republic of China
[14]Huangshan College, Huangshan 245000, People's Republic of China
[15]Huazhong Normal University, Wuhan 430079, People's Republic of China
[16]Hunan University, Changsha 410082, People's Republic of China
[17]Indiana University, Bloomington, Indiana 47405, USA
[18]INFN Laboratori Nazionali di Frascati, Frascati, Italy
[19]Johannes Gutenberg University of Mainz, 55099 Mainz, Germany
[20]Joint Institute for Nuclear Research, 141980 Dubna, Russia
[21]KVI/University of Groningen, 9747 AA Groningen, Netherlands
[22]Lanzhou University, Lanzhou 730000, People's Republic of China
[23]Liaoning University, Shenyang 110036, People's Republic of China
[24]Nanjing Normal University, Nanjing 210046, People's Republic of China
[25]Nanjing University, Nanjing 210093, People's Republic of China
[26]Nankai University, Tianjin 300071, People's Republic of China
[27]Peking University, Beijing 100871, People's Republic of China
[28]Seoul National University, Seoul, 151-747 Korea
[29]Shandong University, Jinan 250100, People's Republic of China
[30]Shanxi University, Taiyuan 030006, People's Republic of China
[31]Sichuan University, Chengdu 610064, People's Republic of China
[32]Soochow University, Suzhou 215006, People's Republic of China
[33]Sun Yat-Sen University, Guangzhou 510275, People's Republic of China
[34]The Chinese University of Hong Kong, Shatin, N. T., Hong Kong
[35]The University of Hong Kong, Pokfulam, Hong Kong
[36]Tsinghua University, Beijing 100084, People's Republic of China
[37]Universitaet Giessen, 35392 Giessen, Germany
[38]University of Hawaii, Honolulu, Hawaii 96822, USA
[39]University of Minnesota, Minneapolis, Minnesota 55455, USA
[40]University of Rochester, Rochester, New York 14627, USA
[41]University of Science and Technology of China, Hefei 230026, People's Republic of China
[42]University of South China, Hengyang 421001, People's Republic of China
[43]University of the Punjab, Lahore-54590, Pakistan
[44]University of Turin and INFN, Turin, Italy
[45]Wuhan University, Wuhan 430072, People's Republic of China
[46]Zhejiang University, Hangzhou 310027, People's Republic of China
[47]Zhengzhou University, Zhengzhou 450001, People's Republic of China

(Received 23 May 2012; published 24 July 2012)

Using a sample of 106×10^6 $\psi(3686)$ events collected with the BESIII detector at the BEPCII storage ring, we have made the first measurement of the $M1$ transition between the radially excited charmonium S-wave spin-triplet and the radially excited S-wave spin-singlet states: $\psi(3686) \to \gamma\eta_c(2S)$. Analyses of the processes $\psi(3686) \to \gamma\eta_c(2S)$ with $\eta_c(2S) \to K_S^0 K^\pm \pi^\mp$ and $K^+K^-\pi^0$ give an $\eta_c(2S)$ signal with a statistical significance of greater than 10 standard deviations under a wide range of assumptions about the signal and background properties. The data are used to obtain measurements of the $\eta_c(2S)$ mass $(M(\eta_c(2S)) = 3637.6 \pm 2.9_{\rm stat} \pm 1.6_{\rm syst}\ {\rm MeV}/c^2)$, width $(\Gamma(\eta_c(2S)) = 16.9 \pm 6.4_{\rm stat} \pm 4.8_{\rm syst}\ {\rm MeV})$, and the product branching-fraction $(\mathcal{B}(\psi(3686) \to \gamma\eta_c(2S)) \times \mathcal{B}(\eta_c(2S) \to K\bar{K}\pi) = (1.30 \pm 0.20_{\rm stat} \pm 0.30_{\rm syst}) \times 10^{-5})$. Combining our result with a *BABAR* measurement of $\mathcal{B}(\eta_c(2S) \to K\bar{K}\pi)$, we find the branching fraction of the $M1$ transition to be $\mathcal{B}(\psi(3686) \to \gamma\eta_c(2S)) = (6.8 \pm 1.1_{\rm stat} \pm 4.5_{\rm syst}) \times 10^{-4}$.

DOI: 10.1103/PhysRevLett.109.042003 PACS numbers: 13.25.Gv, 13.20.Gd, 14.40.Pq

The quarkonium states play an important role in understanding the strong interaction between quarks. The charmonium states below the open-charm production threshold are relatively well understood, with the notable exception of the spin singlets [1], which include the P-wave state h_c and the S-wave ground state η_c and its first radial excitation $\eta_c(2S)$ [2]. These are experimentally challenging because of the low production rates and spin-parity quantum numbers that are inaccessible in direct e^+e^- annihilations.

The $\eta_c(2S)$ was first observed by the Belle collaboration in the process $B^\pm \to K^\pm \eta_c(2S)$, $\eta_c(2S) \to K_S^0 K^\pm \pi^\mp$ [3]. It was confirmed in the two-photon production of

$K_S^0 K^\pm \pi^\mp$ [4,5], and in the double-charmonium production process $e^+e^- \to J/\psi c\bar{c}$ [6,7]. Combining the world-average values [2] with the most recent results from Belle and *BABAR* on two-photon fusion into hadronic final states other than $K_S^0 K^\pm \pi^\mp$ [8,9], one obtains updated averages of the $\eta_c(2S)$ mass and width of 3637.7 ± 1.3 MeV/c^2 and 10.4 ± 4.2 MeV, respectively.

The production of the $\eta_c(2S)$ through a radiative transition from the $\psi(3686)$ requires a charmed-quark spin-flip and, thus, proceeds via a magnetic dipole ($M1$) transition. The branching fraction has been calculated by many authors, with predictions in the range $\mathcal{B}(\psi(3686) \to \gamma\eta_c(2S)) = (0.1\text{–}6.2) \times 10^{-4}$ [10]. A recent calculation [11] that includes contributions from loops containing meson pairs finds a strong cancellation that results in a partial width of (0.08 ± 0.03) keV and a branching fraction of $(2.6 \pm 1.0) \times 10^{-4}$, while a calculation using the light-front quark model and a $2S$ state harmonic oscillator wave function to present the $2S$ charmonium state gives a transition rate of 3.9×10^{-4} [12]. Experimentally, this transition has been searched for by Crystal Ball [13], BES [14], CLEO [15] and most recently by BESIII through $\eta_c(2S) \to VV$ [16]. No convincing signal was observed in any of these searches.

In this Letter, we report the first observation of $\psi(3686) \to \gamma\eta_c(2S)$, with $\eta_c(2S) \to K_S^0 K^\pm \pi^\mp$ and $K^+K^-\pi^0$. The data sample for this analysis consists of an integrated luminosity of 156 pb^{-1} (106×10^6 events) produced at the peak of the $\psi(3686)$ resonance [17] and collected in the BESIII detector [18]. An additional 42 pb^{-1} of data were collected at a center-of-mass energy of $\sqrt{s} = 3.65$ GeV to determine nonresonant continuum background contributions.

The BESIII detector, described in detail in Ref. [18], has an effective geometrical acceptance of 93% of 4π. A small-cell, helium-based main drift chamber in a 1-T magnetic field provides a charged-particle momentum resolution of 0.5% at 1 GeV/c, and specific-ionization (dE/dx) measurements for particle identification with a resolution better than 6% for electrons from Bhabha scattering. The cesium iodide electromagnetic calorimeter (EMC) measures photon energies with resolutions at 1.0 GeV of 2.5% and 5% in the detector's barrel ($|\cos\theta| < 0.8$, where θ is the polar angle with respect to the e^+ direction) and end caps ($0.86 < |\cos\theta| < 0.92$), respectively. Additional particle identification is provided by a time-of-flight system with a time resolution of 80 ps (110 ps) for the barrel (end caps).

Reconstructed charged tracks other than daughters of K_S^0 candidates are required to pass within 1 cm of the e^+e^- annihilation interaction point transverse to the beam line and within 10 cm of the interaction point along the beam axis. Each track is required to have a good-quality fit and to satisfy the condition $|\cos\theta| < 0.93$. Charged-particle identification (PID) is based on combining the dE/dx and time-of-flight information to construct a $\chi^2_{\rm PID}(i)$. The values $\chi^2_{\rm PID}(i)$ and the corresponding confidence levels ${\rm Prob}_{\rm PID}(i)$ are calculated for each charged track for each particle hypothesis i (pion, kaon or proton).

A neutral cluster in the EMC must satisfy fiducial and shower-quality requirements to be accepted as a good photon candidate. Showers must have a minimum energy of 25 MeV and be detected in either the barrel or end cap regions, as previously defined. EMC timing requirements are used to suppress noise and energy deposits unrelated to the event.

In selecting $\gamma K_S^0 K^\pm \pi^\mp$ ($\gamma K^+K^-\pi^0$) events, the decay signal $K_S^0 \to \pi^+\pi^-$ ($\pi^0 \to \gamma\gamma$) is used to tag K_S^0 (π^0). Candidate events must therefore have exactly four (two) charged tracks with zero net charge and at least one (three) good photon(s) for the $\gamma K_S^0 K^\pm \pi^\mp$ ($\gamma K^+K^-\pi^0$) decay mode.

K_S^0 candidates are selected with secondary-vertex fits to all pairs of oppositely charged tracks in the event, assuming pion masses. The combination with the best fit quality is chosen and the event is kept for further analysis if the invariant mass is within 7 MeV/c^2 of the expected K_S^0 mass, and the secondary vertex is at least 0.5 cm from the interaction point. To suppress $\gamma K_S^0 K_S^0$ events, the remaining tracks are required not to form a good K_S^0 candidate. The fitted K_S^0 information is used as input for the subsequent kinematic fit of the complete event.

The $\gamma K_S^0 K^\pm \pi^\mp$ candidates are then subjected to a four-constraint (4C) kinematic fit, with the constraints provided by four-momentum conservation. The discrimination of charge-conjugate channels ($K_S^0 K^+\pi^-$ or $K_S^0 K^-\pi^+$) and the selection of the best photon among multiple candidates are achieved by minimizing $\chi^2 = \chi^2_{\rm 4C} + \chi^2_{\rm PID}(K) + \chi^2_{\rm PID}(\pi)$, where $\chi^2_{\rm 4C}$ is the chi square of the 4C kinematic fit. Events with $\chi^2_{\rm 4C} < 50$ are accepted as $\gamma K_S^0 K^\pm \pi^\mp$ candidates. For $\gamma K^+K^-\pi^0$ candidates, both charged tracks must satisfy the criterion that the kaon-hypothesis probability ${\rm Prob}_{\rm PID}(K)$ is larger than both 0.001 and the probability of any other hypothesis. A five-constraint (5C) kinematic fit, with the π^0 mass as the additional constraint, is used to select the best transition photon and the $\pi^0 \to \gamma\gamma$ combination. Events with $\chi^2_{\rm 5C} < 30$ are accepted as $\gamma K^+K^-\pi^0$ candidates.

We use the program LUNDCRM [19] to generate inclusive Monte Carlo (MC) events for background studies. The signal is generated with the expected angular distribution for $\psi(3686) \to \gamma\eta_c(2S)$, and the subsequent $\eta_c(2S) \to K_S^0 K^\pm \pi^\mp$ and $K^+K^-\pi^0$ decays are generated according to phase space. The detector response is simulated with a GEANT4-based package [20] that has been tuned to match the performance of the detector components.

The $\psi(3686) \to \gamma\eta_c(2S)$, $\eta_c(2S) \to K_S^0 K^\pm \pi^\mp (K^+K^-\pi^0)$ signal suffers significantly from background contributions from leptonic J/ψ decays and $J/\psi \to K^+K^-$ in $\psi(3686) \to \pi^+\pi^- J/\psi$, and $\psi(3686) \to \eta J/\psi$ with

$\eta \to \pi^+\pi^-\pi^0$ $(\gamma\gamma)$. For the $\gamma K_S^0 K^\pm \pi^\mp$ channel, these background contributions are suppressed by requiring that the recoil mass of all $\pi^+\pi^-$ pairs be less than 3.05 GeV/c^2. For the $\gamma K^+K^-\pi^0$ channel, this type of contamination is removed by requiring that the invariant mass of the two charged tracks, assuming they are muons, be less than 2.9 GeV/c^2. The remaining dominant background sources are (1) $\psi(3686) \to K_S^0 K^\pm \pi^\mp$ $(K^+K^-\pi^0)$ events with a fake photon candidate; (2) events with the same final states including $K_S^0 K^\pm \pi^\mp \gamma_{\rm ISR/FSR}$ $(K^+K^-\pi^0\gamma_{\rm ISR/FSR})$ with the photon from initial- or final-state radiation (ISR, FSR) and $\psi(3686) \to \omega K^+K^-$ with $\omega \to \gamma\pi^0$; and (3) events with an extra photon, primarily from $\psi(3686) \to \pi^0 K_S^0 K^\pm \pi^\mp$ $(\pi^0 K^+K^-\pi^0)$ with $\pi^0 \to \gamma\gamma$. MC studies demonstrate that contributions from all other known processes are negligible.

The events in the first category, with a fake photon incorporated into the kinematic fit, produce a peak in the $K_S^0 K^\pm \pi^\mp$ $(K^+K^-\pi^0)$ mass spectrum close to the expected $\eta_c(2S)$ mass, with a sharp cutoff due to the 25-MeV photon-energy threshold.

Because the fake photon adds no information to the fit, its inclusion distorts the mass measurement. We therefore determine the mass from a modified kinematic fit in which the magnitude of the photon momentum is allowed to freely float (3C for $\gamma K_S^0 K^\pm \pi^\mp$ and 4C for $\gamma K^+K^-\pi^0$). In the case of a fake photon, the momentum tends to zero, which improves the background separation with minimal distortion of the signal line shape [16].

Background contributions from $\psi(3686) \to K_S^0 K^\pm \pi^\mp$ $(K^+K^-\pi^0)$ and $\psi(3686) \to K_S^0 K^\pm \pi^\mp \gamma_{\rm FSR}$ $(K^+K^-\pi^0\gamma_{\rm FSR})$ are estimated with MC distributions for those processes normalized according to a previous measurement of the branching ratios [21]. FSR is simulated in our MC generations with PHOTOS [22], and the FSR contribution is scaled by the ratio of the FSR fractions in data and MC generations for a control sample of $\psi(3686) \to \gamma\chi_{cJ}$ $(J = 0$ or $1)$ events. For this study the χ_{cJ} is selected in three final states with or without an extra FSR photon, namely $K_S^0 K^\pm \pi^\mp(\gamma_{\rm FSR})$, $\pi^+\pi^-\pi^+\pi^-(\gamma_{\rm FSR})$, and $\pi^+\pi^- K^+K^-(\gamma_{\rm FSR})$, as described in Ref. [16]. Background contributions from the continuum process $e^+e^- \to \gamma^* \to K_S^0 K^\pm \pi^\mp(\gamma_{\rm FSR})$ $(K^+K^-\pi^0(\gamma_{\rm FSR}))$ and the ISR process $e^+e^- \to \gamma^*\gamma_{\rm ISR} \to K_S^0 K^\pm \pi^\mp \gamma_{\rm ISR}(K^+K^-\pi^0\gamma_{\rm ISR})$ are estimated with data collected at $\sqrt{s} = 3.65$ GeV corrected for differences in the integrated luminosity and the cross section, and with particle momenta and energies scaled to account for the beam-energy difference. MC simulations show that the $K_S^0 K^\pm \pi^\mp$ $(K^+K^-\pi^0)$ mass spectra are similar for FSR and ISR events. Events without radiation have the same mass distribution independently of originating from a resonant $\psi(3686)$ decay or from the nonresonant continuum production. Thus, the background shapes from $K_S^0 K^\pm \pi^\mp(K^+K^-\pi^0)$ and $K_S^0 K^\pm \pi^\mp \gamma_{\rm ISR/FSR}(K^+K^-\pi^0\gamma_{\rm ISR/FSR})$ are described by the sum of the MC-simulated $K_S^0 K^\pm \pi^\mp(K^+K^-\pi^0)$ and $K_S^0 K^\pm \pi^\mp \gamma_{\rm FSR}(K^+K^-\pi^0\gamma_{\rm FSR})$ invariant-mass shapes, with the proportions fixed according to the procedure described above. The shapes of background mass distributions from $\psi(3686) \to \omega K^+K^-$ with $\omega \to \gamma\pi^0$ are parameterized with a double-Gaussian function, and its level is measured with the same data sample and fixed in the final fit.

The third type of background, that with an extra photon, $\pi^0 K_S^0 K^\pm \pi^\mp(\pi^0 K^+K^-\pi^0)$, is measured with data and normalized according to the simulated contamination rate. It contributes a smooth component around the χ_{cJ} $(J = 1, 2)$ mass region with a small tail in the $\eta_c(2S)$ signal region that is described by a Novosibirsk function [23] (Gaussian function) for the $\pi^0 K_S^0 K^\pm \pi^\mp$ $(\pi^0 K^+K^-\pi^0)$ background. The shape and size of this background is fixed in the fit.

The mass spectra for the $K_S^0 K^\pm \pi^\mp$ and $K^+K^-\pi^0$ channels are fitted simultaneously to extract the yield, mass, and width of $\eta_c(2S)$. To better determine the background and mass resolution from the data, the mass spectra are fitted over a range (3.46–3.71 GeV/c^2) that includes the χ_{c1} and χ_{c2} resonances as well as the $\eta_c(2S)$ signal. The final mass spectra and the likelihood fit results are shown in Fig. 1. Each fitting function includes four components, namely, $\eta_c(2S)$, χ_{c1}, χ_{c2}, and the summed background described above. Line shapes for χ_{c1} and χ_{c2} are obtained from MC simulations and convolved with Gaussian functions to

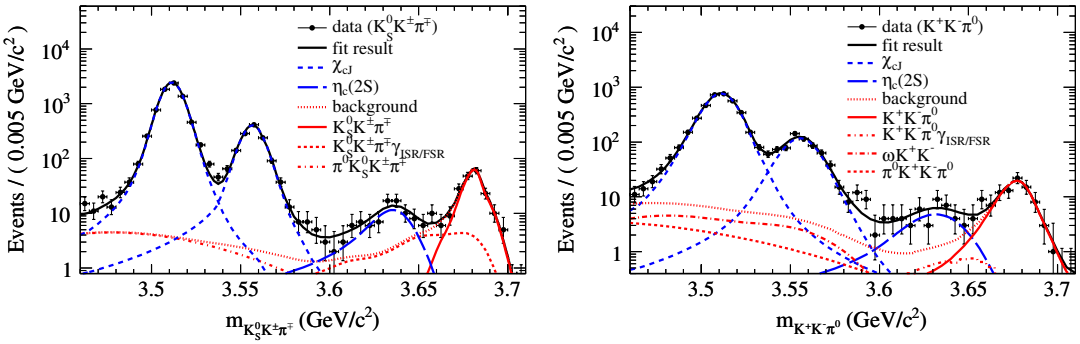

FIG. 1 (color online). The invariant-mass spectrum for $K_S^0 K^\pm \pi^\mp$ (left panel), $K^+K^-\pi^0$ (right panel), and the simultaneous likelihood fit to the three resonances and combined background sources as described in the text.

accommodate the mass-scale and resolution differences from data. For both modes, the χ_{c1} and χ_{c2} widths are fixed to the PDG values [2]. Based on MC studies, the mass shift and resolution for the resonances are found to vary linearly as a function of the $K^0_S K^\pm \pi^\mp (K^+K^-\pi^0)$ invariant mass. These parameters are extrapolated from χ_{c1} and χ_{c2} to $\eta_c(2S)$.

The line shape for the $\eta_c(2S)$ produced in the $M1$ transition of the $\psi(3686)$ is assumed to have the form $[E_\gamma^3 \times \mathrm{BW}(m) \times f_d(E_\gamma) \times \epsilon(m)] \otimes G(\delta m, \sigma)$, where m is the invariant mass of $K^0_S K^\pm \pi^\mp$ or $K^+K^-\pi^0$, $E_\gamma = (m^2_{\psi(3686)} - m^2)/2m_{\psi(3686)}$ is the energy of the transition photon in the rest frame of $\psi(3686)$, BW(m) is the Breit-Wigner function for $\eta_c(2S)$, $f_d(E_\gamma)$ is a function that damps the diverging tail originating from the E_γ^3 dependence, $\epsilon(m)$ is the mass-dependent efficiency function determined by a full simulation of the signal, and $G(\delta m, \sigma)$ is a Gaussian function describing the mass shift and the detector resolution. For the damping function we use a functional form introduced by the KEDR collaboration [24]: $f_d = E_0^2/[E_\gamma E_0 + (E_\gamma - E_0)]^2$, where $E_0 = (m^2_{\psi(3686)} - m^2_{\eta_c(2S)})/2m_{\psi(3686)}$ is the peak energy of the transition photon. To assess the sensitivity of our results to the choice of this function, we also consider an alternative form used by CLEO [25]: $f_d = \exp(-\frac{E_\gamma^2}{8\beta^2})$, with CLEO's fitted value of $\beta = (65.0 \pm 2.5)$ MeV.

The fit shown in Fig. 1 has a χ^2 of 72 for 79 degrees of freedom. The results for the yields of $\eta_c(2S)$ events are 81 ± 14 for the $K^0_S K^\pm \pi^\mp$ channel and 46 ± 11 for the $K^+K^-\pi^0$ channel. Consistent yields are found for separate fits to the two channels [26]. The $K^0_S K^\pm \pi^\mp$ channel determines primarily the precision for the $\eta_c(2S)$ mass and width measurements in the simultaneous fit with the results $M_{\eta_c(2S)} = 3637.6 \pm 2.9$ MeV$/c^2$ and $\Gamma_{\eta_c(2S)} = 16.9 \pm 6.4$ MeV, respectively. The combined statistical significance of the signal in the two modes is 11.1σ, which is obtained by comparing the likelihoods of the fits with and without the $\eta_c(2S)$ signal. The robustness of this result was tested by considering variations of the resonant line shapes, background assumptions, and other systematic effects. In all the cases, the statistical significance is found to be larger than 10.2σ.

Combining the observed number of signal events with the efficiencies of 25.6% and 20.2% for the $K^0_S K^\pm \pi^\mp$ and $K^+K^-\pi^0$ final states, respectively, from full simulations of the signal with the measured $\eta_c(2S)$ mass and width, we find the product branching fractions $\mathcal{B}(\psi(3686) \to \gamma\eta_c(2S)) \times \mathcal{B}(\eta_c(2S) \to K^0_S K^\pm \pi^\mp) = (4.31 \pm 0.75) \times 10^{-6}$, and $\mathcal{B}(\psi(3686) \to \gamma\eta_c(2S)) \times \mathcal{B}(\eta_c(2S) \to K^+K^-\pi^0) = (2.17 \pm 0.52) \times 10^{-6}$, where the errors are statistical only. The ratio of the branching fractions agrees well with the isospin symmetry expectation of 2:1 between $K^0_S K^\pm \pi^\mp$ and $K^+K^-\pi^0$. The product branching fraction for $\psi(3686) \to \gamma\eta_c(2S)$, $\eta_c(2S) \to K\bar{K}\pi$ can be obtained by doubling the sum of the $K^0_S K^\pm \pi^\mp$ and $K^+K^-\pi^0$ branching fractions to obtain $\mathcal{B}(\psi(3686) \to \gamma\eta_c(2S)) \times \mathcal{B}(\eta_c(2S) \to K\bar{K}\pi) = (1.30 \pm 0.20) \times 10^{-5}$, where the error takes into account the correlation between the two measured branching fractions from the simultaneous fit.

The systematic uncertainties in the branching fraction, $\eta_c(2S)$ mass, and $\eta_c(2S)$ width measurements are summarized in Table I. The uncertainties due to the choice of the background shape, the damping function, the fitting range, and the linear extrapolated mass shift for $\eta_c(2S)$ are common among the three measurements and are determined together. The systematic errors in the mass and width due to the $K^0_S K^\pm \pi^\mp(\gamma_{\mathrm{ISR/FSR}})$ $(K^+K^-\pi^0(\gamma_{\mathrm{ISR/FSR}}))$ background shape are evaluated by changing the relative ratio of the $K^0_S K^\pm \pi^\mp$ $(K^+K^-\pi^0)$ background events with and without radiation. The uncertainties from the $\pi^0 K^0_S K^\pm \pi^\mp$ $(\pi^0 K^+K^-\pi^0)$ background shape are estimated by changing the function parameterizing the measured mass spectrum. The uncertainty due to the choice of damping function is estimated from the difference between results obtained with the default (KEDR) and alternative (CLEO) functional forms. The uncertainties due to the choice of fitting range are estimated by taking the largest differences between results found with the standard fitting range and those obtained using alternative ranges. The uncertainties from the linear extrapolation of the mass shifts from χ_{c1} and χ_{c2} to $\eta_c(2S)$ are estimated from the maximum changes in the fitting results obtained by varying the mass shifts within their errors.

The branching-fraction measurement is affected by additional effects that enter through the yield determination, including those associated with charged-particle tracking, photon reconstruction, particle identification, K^0_S reconstruction, and kinematic fitting (χ^2 requirement), all of which are estimated with control samples in the data [27].

TABLE I. The absolute systematic uncertainties in the $\eta_c(2S)$ mass (in MeV$/c^2$), width (in MeV) and the relative systematic error (in %) in $\mathcal{BB}$, the product branching fraction $\mathcal{B}(\psi(3686) \to \gamma\eta_c(2S)) \times \mathcal{B}(\eta_c(2S) \to K\bar{K}\pi)$, measurements.

Source	Mass	Width	$\mathcal{BB}$
Background shape	1.3	2.6	9.9
Damping function	0.7	4.0	19.6
Fitting range	0.1	0.4	1.3
Mass shift	0.6	0.2	0.4
Tracking	···	···	4.0
Photon reconstruction	···	···	1.3
Particle identification	···	···	1.3
K^0_S reconstruction	···	···	2.3
Kinematic fitting	···	···	3.9
$\eta_c(2S)$ decay dynamics	···	···	1.5
Number of $\psi(3686)$ events	···	···	4.0
Total	1.6	4.8	23.3

The effect of the uncertainty in the dynamics of the decay $\eta_c(2S) \to K_S^0 K^\pm \pi^\mp (K^+ K^- \pi^0)$, which is treated as phase space in our default signal MC sample, is estimated with an alternative MC sample replicating the Dalitz distribution of $\eta_c(2S) \to K_S^0 K^\pm \pi^\mp$ decay recently measured by the Belle collaboration [28]. A 0.8% (3.0%) relative difference in the efficiency was found between the default and alternative MC samples for $K_S^0 K^\pm \pi^\mp$ $(K^+ K^- \pi^0)$, leading to a 1.5% difference in the total branching ratio, which we take as a systematic error. Finally, there is an overall 4% uncertainty in the branching fraction associated with the determination of the total number of $\psi(3686)$ events in our data sample [17].

We assume that all the sources of systematic uncertainties are independent and combine them in quadrature to obtain the overall systematic uncertainties given in Table I. The total systematic uncertainties in the mass and width measurements are 1.6 MeV/c^2 and 4.8 MeV, respectively; the total relative systematic uncertainty in the product branching fraction $\mathcal{B}(\psi(3686) \to \gamma\eta_c(2S)) \times \mathcal{B}(\eta_c(2S) \to K\bar{K}\pi)$ is 23.3%. Using the measurement of $\mathcal{B}(\eta_c(2S) \to K\bar{K}\pi) = (1.9 \pm 0.4 \pm 1.1)\%$ from the *BABAR* experiment [29], we find an $M1$-transition branching fraction of $\mathcal{B}(\psi(3686) \to \gamma\eta_c(2S)) = (6.8 \pm 1.1 \pm 4.5) \times 10^{-4}$, where the systematic error is dominated by that of the *BABAR* result.

In summary, we report the first observation of the $M1$ transition $\psi(3686) \to \gamma\eta_c(2S)$ through the decay processes $\psi(3686) \to \gamma K_S^0 K^\pm \pi^\mp$ and $\gamma K^+ K^- \pi^0$. We measure the mass of the $\eta_c(2S)$ to be $3637.6 \pm 2.9 \pm 1.6$ MeV/c^2, the width $16.9 \pm 6.4 \pm 4.8$ MeV, and the product branching fractions $\mathcal{B}(\psi(3686) \to \gamma\eta_c(2S)) \times \mathcal{B}(\eta_c(2S) \to K\bar{K}\pi) = (1.30 \pm 0.20 \pm 0.30) \times 10^{-5}$, where the quoted uncertainties are statistical and systematic, respectively. The main systematic limitations to these measurements arise from the choice of the functional form for the damping factor in the $\eta_c(2S)$ line shape and from uncertainty in the choice of the background line shapes. Where previously published values and limits exist our results are consistent with those, and the branching-fraction measurement of the $M1$ transition $\psi(3686) \to \gamma\eta_c(2S)$ of $(6.8 \pm 1.1 \pm 4.5) \times 10^{-4}$ agrees with theoretical calculations and naive estimates based on the $J/\psi \to \gamma\eta_c$ transition [15].

We would like to thank S. Eidelman and A. Vinokurova for supplying the details of the Dalitz plot of $\eta_c(2S) \to K_S^0 K^\pm \pi^\mp$ decay from the Belle experiment. The BESIII collaboration thanks the staff of BEPCII and the computing center for their hard efforts. This work is supported in part by the Ministry of Science and Technology of China under Contract No. 2009CB825200; National Natural Science Foundation of China (NSFC) under Contracts No. 10625524, No. 10821063, No. 10825524, No. 10835001, No. 10935007, No. 11125525; Joint Funds of the National Natural Science Foundation of China under Contracts No. 11079008, No. 11179007; the Chinese Academy of Sciences (CAS) Large-Scale Scientific Facility Program; CAS under Contracts No. KJCX2-YW-N29, No. KJCX2-YW-N45; 100 Talents Program of CAS; Istituto Nazionale di Fisica Nucleare, Italy; U. S. Department of Energy under Contracts No. DE-FG02-04ER41291, No. DE-FG02-91ER40682, No. DE-FG02-94ER40823; U.S. National Science Foundation; University of Groningen (RuG); the Helmholtzzentrum fuer Schwerionenforschung GmbH (GSI), Darmstadt and the WCU Program of National Research Foundation of Korea under Contract No. R32-2008-000-10155-0.

*Also at the Moscow Institute of Physics and Technology, Moscow, Russia.
†On leave from the Bogolyubov Institute for Theoretical Physics, Kiev, Ukraine.
‡Also at the University of Piemonte Orientale and INFN (Turin), USA.
§Present address: INFN and University of Perugia, I-06100 Perugia, Italy.
‖Also at the PNPI, Gatchina, Russia.
¶Present address: Nagoya University, Nagoya, Japan.
**Present address: Wuhan Electric Power Technical College, Wuhan 430079, People's Republic of China.

[1] For a recent review, see N. Brambilla *et al.*, Eur. Phys. J. C **71**, 1534 (2011).
[2] K. Nakamura *et al.* (Particle Data Group), J. Phys. G **37**, 075021 (2010).
[3] S.-K. Choi *et al.* (Belle Collaboration), Phys. Rev. Lett. **89**, 102001 (2002).
[4] B. Aubert *et al.* (*BABAR* Collaboration), Phys. Rev. Lett. **92**, 142002 (2004).
[5] D. M. Asner *et al.* (CLEO Collaboration), Phys. Rev. Lett. **92**, 142001 (2004).
[6] B. Aubert *et al.* (*BABAR* Collaboration), Phys. Rev. D **72**, 031101 (2005).
[7] K. Abe *et al.* (Belle Collaboration), Phys. Rev. Lett. **89**, 142001 (2002).
[8] P. del Amo Sanchez *et al.* (*BABAR* Collaboration), Phys. Rev. D **84**, 012004 (2011).
[9] H. Nakazawa (for the Belle Collaboration), in Proc. Sci., ICHEP2010 (2010) 162.
[10] See the compilation of the results in K. Gao, arXiv:0909.2812.
[11] G. Li and Q. Zhao, Phys. Lett. B **670**, 55 (2008); , Phys. Rev. D **84**, 074005 (2011).
[12] Tao Peng and Bo-Qiang Ma, Eur. Phys. J. A **48**, 66 (2012).
[13] C. Edwards *et al.* (Crystal Ball Collaboration), Phys. Rev. Lett. **48**, 70 (1982).
[14] C. Z. Yuan, Ph.D thesis, Institute of High Energy Physics, Chinese Academy of Sciences, 1997.
[15] D. Cronin-Hennessy *et al.* (CLEO Collaboration), Phys. Rev. D **81**, 052002 (2010).
[16] M. Ablikim *et al.* (BESIII Collaboration), Phys. Rev. D **84**, 091102 (2011).
[17] M. Ablikim *et al.* (BESIII Collaboration), Phys. Rev. D **81**, 052005 (2010).

[18] M. Ablikim *et al.* (BESIII Collaboration), Nucl. Instrum. Methods Phys. Res., Sect. A **614**, 345 (2010).
[19] J. C. Chen, G. S. Huang, X. R. Qi, D. H. Zhang and Y. S. Zhu, Phys. Rev. D **62**, 034003 (2000).
[20] S. Agostinelli *et al.* (GEANT4 Collaboration), Nucl. Instrum. Methods Phys. Res., Sect. A **506**, 250 (2003).
[21] M. Ablikim *et al.* (BES Collaboration), Phys. Lett. B **614**, 37 (2005).
[22] E. Barberio and Z. Was, Comput. Phys. Commun. **79**, 291 (1994).
[23] The Novosibirsk function is defined as $f(m) = A_S \exp(-0.5\{\ln^2[1+\Lambda\tau(m-m_0)]/\tau^2+\tau^2\})$, where $\Lambda = \sinh(\tau\sqrt{\ln 4})/(\sigma\tau\sqrt{\ln 4})$, the peak position is m_0, the width is σ, and τ is the tail parameter.
[24] V. V. Anashin *et al.*, arXiv:1012.1694.
[25] R. E. Mitchell *et al.* (CLEO Collaboration), Phys. Rev. Lett. **102**, 011801 (2009).
[26] The individual fit of the $K^0_S K^\pm \pi^\mp$ spectrum gives $M_{\eta_c(2S)(K^0_S K^\pm \pi^\mp)} = (3637.0 \pm 2.7)\ \mathrm{MeV}/c^2$, $\Gamma_{\eta_c(2S)(K^0_S K^\pm \pi^\mp)} = (14.4 \pm 5.3)\ \mathrm{MeV}$, $N_{\eta_c(2S)(K^0_S K^\pm \pi^\mp)} = 77 \pm 13$ with a statistical significance of 9.5σ; and the fit of the $K^+K^-\pi^0$ distribution gives $M_{\eta_c(2S)(K^+K^-\pi^0)} = (3656 \pm 31)\ \mathrm{MeV}/c^2$, $\Gamma_{\eta_c(2S)(K^+K^-\pi^0)} = (60 \pm 39)$ MeV, $N_{\eta_c(2S)(K^+K^-\pi^0)} = 72 \pm 32$ with a statistical significance of 5.7σ.
[27] M. Ablikim *et al.* (BESIII Collaboration), Phys. Rev. D **83**, 112005 (2011).
[28] A. Vinokurova *et al.* (Belle Collaboration), Phys. Lett. B **706**, 139 (2011).
[29] B. Aubert *et al.* (*BABAR* Collaboration), Phys. Rev. D **78**, 012006 (2008).